

# Short-Range Structure of Invert Glasses along the Pseudo-Binary Join $\text{MgSiO}_3\text{--Mg}_2\text{SiO}_4$ : Results from $^{29}\text{Si}$ and $^{25}\text{Mg}$ MAS NMR Spectroscopy

S. Sen,<sup>\*,†</sup> H. Maekawa,<sup>‡</sup> and G. N. Papatheodorou<sup>§</sup>

Department of Chemical Engineering & Materials Science, University of California at Davis, Davis, California 95616, Graduate School of Engineering, Tohoku University, Aoba-ku, Sendai, 980-8579, Japan, and Institute of Chemical Engineering and High Temperature Chemical Processes FORTH, P.O. Box 1414, GR-26504, Patras, Greece

Received: August 17, 2009; Revised Manuscript Received: October 2, 2009

The short-range structure of “invert” glasses along the pseudobinary join  $\text{MgSiO}_3\text{--Mg}_2\text{SiO}_4$  has been studied using  $^{29}\text{Si}$  and  $^{25}\text{Mg}$  MAS NMR spectroscopy. The results indicate a progressive compositional evolution in Q speciation that approximately follows a statistical distribution. The  $\text{Mg}_2\text{SiO}_4$  glass shows an abrupt deviation from this trend with the presence of nearly 40% of the Si atoms as  $(\text{Si}_2\text{O}_7)^{6-}$  dimers, i.e.,  $\text{Q}^1$  species.  $\text{Mg}^{2+}$  ions are present in predominantly octahedral coordination in all glasses. When taken together, these results indicate that glasses with MgO contents between 50 and 60 mol % are characterized by a structure consisting primarily of at least three types of Q species and  $\text{MgO}_6$  octahedra. On the other hand, the structure of glasses with >60 mol % MgO appears to consist of  $\text{Q}^0$  and  $\text{Q}^1$  species with structural connectivity being primarily provided by the  $\text{MgO}_6$  octahedra. The possible consequences of such compositional evolution of structure on the ability of glass formation in this system are discussed.

## I. Introduction

Knowledge of structure and structure-property relationships in silicate glasses and melts is important in earth and materials sciences and has important ramifications for processes as diverse as manufacturing of glasses and glass-ceramics and volcanic eruption.<sup>1–5</sup> Magnesium-rich silicates are one of the most important constituents of the terrestrial and lunar mantles and meteorites.<sup>1</sup> On the other hand, melt-grown  $\text{Cr}^{4+}$ -doped  $\text{Mg}_2\text{SiO}_4$  (forsterite) crystals have shown significant potential for application as laser materials.<sup>5</sup> A number of spectroscopic and diffraction studies of the structures of  $\text{MgO--SiO}_2$  binary glasses have been reported in the literature over the past several decades.<sup>2</sup> The so-called “invert” glasses in the  $\text{MgO--SiO}_2$  binary system with  $\leq 50$  mol %  $\text{SiO}_2$  have recently received significant attention as the glass-forming region has been extended down to the orthosilicate  $\text{Mg}_2\text{SiO}_4$  composition with 33.33 mol %  $\text{SiO}_2$  using containerless levitation techniques and  $\text{CO}_2$  laser melting.<sup>6–13</sup> Systematic structural studies of these invert glasses are particularly interesting, as they can provide the clue to their glass-forming ability at such low concentrations of the nominal network-former  $\text{SiO}_2$ . Unfortunately, the results of the structural studies of these glasses have remained contradictory and significantly controversial.

Detailed composition dependent structural evolution of invert  $\text{MgO--SiO}_2$  glasses has been studied by neutron and X-ray diffraction by Wilding and co-workers<sup>6,7</sup> and more recently using Raman spectroscopy by Papatheodorou and co-workers.<sup>8</sup> The diffraction studies indicate that the structure of these glasses evolves from a sparse network of bridged  $\text{SiO}_4$  tetrahedra and a mixture of  $\text{MgO}_4$  and  $\text{MgO}_5$  polyhedra near the  $\text{MgSiO}_3$  composition to a percolation domain of  $\text{MgO}_x$  ( $x = 4, 5, 6$ )

polyhedra and isolated  $\text{SiO}_4$  units ( $\text{Q}^0$  species) near the  $\text{Mg}_2\text{SiO}_4$  composition. The coordination number of Mg is suggested to increase abruptly from  $\sim 4.5$  near the  $\text{MgSiO}_3$  composition to  $\sim 5.0$  near the  $\text{Mg}_2\text{SiO}_4$  composition.<sup>6,7</sup> On the other hand, Raman spectroscopic results have indicated the presence of bridging oxygens in all glasses and a more gradual evolution of structure and Q speciation in these glasses as a function of composition.<sup>8</sup> It may be noted that the structural and chemical local order within the network in silicate glasses can be characterized by the concentration of various types of Si environments, typically denoted as  $\text{Q}^n$  species, where  $n$  varies between 0 and 4 and denotes the number of bridging oxygens. Further insight into the structure of invert  $\text{MgO--SiO}_2$  glasses can be gained if one considers the results of recent  $^{29}\text{Si}$  and  $^{25}\text{Mg}$  nuclear magnetic resonance (NMR) spectroscopic studies of  $\text{MgSiO}_3$  and  $\text{Mg}_2\text{SiO}_4$  glasses.<sup>11,13</sup> Simulation of the static  $^{29}\text{Si}$  NMR spectrum of  $\text{Mg}_2\text{SiO}_4$  glass has shown the presence of nearly 40% of the Si atoms as  $(\text{Si}_2\text{O}_7)^{6-}$  dimers, consistent with the Raman spectroscopic results.<sup>11</sup> The nominal composition of this glass demands the presence of only  $\text{Q}^0$  species, and hence, formation of dimers would release “free” oxygens that are not bonded to any Si atom. It has been speculated that these “free” oxygens will be coordinated to Mg, resulting in an abrupt increase in Mg coordination number. This scenario is consistent with the Mg coordination numbers obtained by Wilding and co-workers on the basis of diffraction data, as mentioned above. On the other hand,  $^{25}\text{Mg}$  magic-angle-spinning (MAS) NMR and triple-quantum (3Q) MAS NMR spectra have been interpreted to be resulting from Mg being in octahedral coordination with oxygen in the  $\text{MgSiO}_3$  glass with a range of distorted geometries.<sup>12,13</sup> A combined X-ray diffraction and reverse Monte Carlo simulation study of the structure of  $\text{Mg}_2\text{SiO}_4$  glass has estimated the relative fractions of  $\text{MgO}_4$ ,  $\text{MgO}_5$ , and  $\text{MgO}_6$  polyhedra to be  $\sim 30$ ,  $50$ , and  $20\%$ , respectively, resulting in an average Mg coordination number of  $\sim 5$ .<sup>10</sup> On the basis of these results, Shimoda et al.<sup>12</sup> have hypothesized that the Mg

\* Corresponding author.

<sup>†</sup> University of California at Davis.

<sup>‡</sup> Tohoku University.

<sup>§</sup> Institute of Chemical Engineering and High Temperature Chemical Processes FORTH.

coordination number actually decreases along the pseudobinary  $\text{MgSiO}_3$ – $\text{Mg}_2\text{SiO}_4$  join with increasing Mg concentration. Such a decrease results from the requirement of the formation of  $\text{MgO}_4$  tetrahedra as additional network formers besides the  $\text{SiO}_4$  tetrahedra for the stabilization of the  $\text{Mg}_2\text{SiO}_4$  glass. It should be noted that this structural hypothesis is in strong contrast to the scenario proposed by Wilding and co-workers based on an abrupt increase in the Mg coordination number near the  $\text{Mg}_2\text{SiO}_4$  composition (*vide supra*).

We report here the results of a systematic  $^{29}\text{Si}$  and  $^{25}\text{Mg}$  MAS NMR spectroscopic study of nine glasses along the pseudobinary  $\text{MgSiO}_3$ – $\text{Mg}_2\text{SiO}_4$  join, prepared using levitation and  $\text{CO}_2$  laser heating methods. The purpose of the present work is to investigate the compositional evolution of the short-range structure of these glasses to test the validity of the various structural models proposed in the literature.

## II. Experimental Section

**Sample Synthesis.** The starting chemicals for the preparation of the glasses were reagent grade  $\text{MgO}$  (Alfa Aesar, 99.95%) and  $\text{SiO}_2$  (Alfa Aesar, 99.999% puratronic grade). The oxides were first dried by heating in a neutral atmosphere to up to  $\sim 400^\circ\text{C}$  and were then transferred into a dry glovebox. Powder mixtures corresponding to the stoichiometries of  $\text{MgSiO}_3$  and  $\text{Mg}_2\text{SiO}_4$  were first prepared in 5 g quantities. These mixtures were thoroughly ground and pelletized and subsequently partially sintered in a furnace at  $\sim 1000^\circ\text{C}$  for a few days. These pellets were then crushed again inside the glovebox and were used as starting materials for preparing the powder mixtures of intermediate compositions. Approximately 10–20 mg of the powder mixtures were melted in a water-cooled copper hearth using a 240 W continuous wave  $\text{CO}_2$  laser (Synrad, Evolution Series) operating at a wavelength of  $10.6\ \mu\text{m}$ . Only a small percentage ( $<15\%$ ) of the laser power was used to avoid evaporation of the oxides and reaching temperatures far above the liquidus. Polycrystalline, nearly spherical, white samples were thus obtained after turning off the laser. These samples were then levitated in Ar gas flow through a conical nozzle and heated and melted using the  $\text{CO}_2$  laser. Finally, glasses were obtained by rapid melt-quenching via sudden shut down of the laser. Multiple spheres of  $\sim 1\ \text{mm}$  diameter were prepared this way, amounting to a total of nearly 100 mg for each composition, except the  $\text{MgSiO}_3$  composition for which nearly 300 mg sample was made available, for  $^{29}\text{Si}$  and  $^{25}\text{Mg}$  MAS NMR spectroscopy. The homogeneity and purity of such glasses synthesized in a similar fashion had been confirmed in previous works by others.<sup>6,9,10</sup> The compositions of the glass spheres used in this study were checked using atomic absorption spectroscopy as well as by energy dispersive spectroscopy. The compositions of all samples were found to be within  $\pm 1\ \text{wt}\%$  of the nominal composition.

**MAS NMR Spectroscopy.** The  $^{29}\text{Si}$  MAS NMR spectra of all glass samples were collected with a 4 mm Bruker MAS probe and a Bruker Avance 500 spectrometer equipped with a wide bore ultrashield magnet operating at a Larmor frequency of 99.3 MHz for  $^{29}\text{Si}$ . The samples in the form of spherical beads were spun in  $\text{ZrO}_2$  rotors at 10 kHz without further crushing. All one-pulse  $^{29}\text{Si}$  MAS spectra were collected using a radio frequency (rf) pulse of duration  $1.5\ \mu\text{s}$  (corresponding to a  $45^\circ$  tip angle) and with a recycle delay of 60 s. Approximately 3000 free induction decays (FIDs) were averaged to obtain each spectrum. Chemical shifts for all  $^{29}\text{Si}$  spectra are referenced in parts per million relative to tetramethylsilane (TMS).

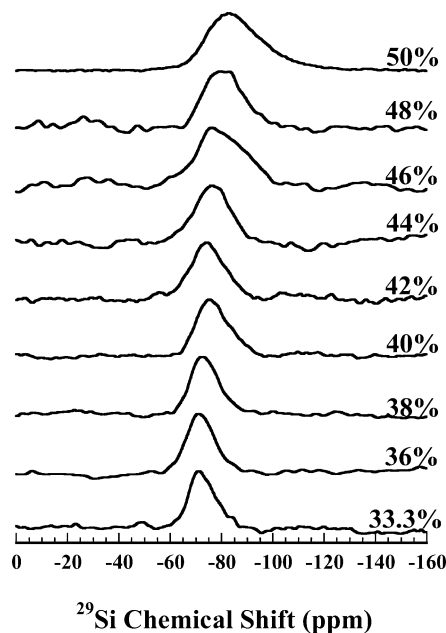


**Figure 1.**  $^{29}\text{Si}$  MAS NMR spectra of  $(\text{MgO})_x(\text{SiO}_2)_{100-x}$  glasses. Corresponding glass compositions are given alongside each spectrum in terms of  $\text{SiO}_2$  content in mol %.

The  $^{25}\text{Mg}$  MAS NMR spectra of select glass samples were acquired using a JNM-ECA930 (JEOL) spectrometer equipped with a JEOL magnet (21.8 T) operating at a Larmor frequency of 56.8 MHz for  $^{25}\text{Mg}$ . All MAS NMR spectra were acquired using a single rf pulse of a duration of  $1\ \mu\text{s}$  (solids  $45^\circ$ ) and a recycle delay of 1 s. Samples were taken in  $\text{Si}_3\text{N}_4$  rotors and were spun at 16 kHz in a 4 mm JEOL MQ/MAS probe. Approximately 80 000 to 168 000 FIDs were averaged to obtain each spectrum. Chemical shifts for all  $^{25}\text{Mg}$  spectra are referenced in parts per million relative to 1 M  $\text{MgCl}_2$  aqueous solution.

## III. Results

The  $^{29}\text{Si}$  MAS NMR spectra for all glasses are shown in Figure 1. The fast sample spinning results in sidebands that are far removed from the position of the main peak and negligible sideband intensities (1% or less). These sidebands are not shown in Figure 1 and have not been included in the line shape simulation process. It is clear that the average  $^{29}\text{Si}$  MAS NMR peak position in these spectra systematically shifts to higher ppm values (i.e., gets deshielded) with increasing  $\text{MgO}$  concentration. This result is consistent with the progressive depolymerization of the silicate network and replacement of  $\text{Q}^2$  and  $\text{Q}^3$  species with  $\text{Q}^1$  and  $\text{Q}^0$  species upon addition of  $\text{MgO}$ . The  $^{29}\text{Si}$  MAS NMR line shape for Mg-silicate glasses is relatively featureless and therefore difficult to simulate without a priori knowledge of the peak positions and widths for the various Q species. Fortunately, the isotropic chemical shifts  $\delta_{\text{iso}}$  for  $\text{Q}^0$ ,  $\text{Q}^1$ , and  $\text{Q}^2$  species in  $\text{MgO}$ – $\text{SiO}_2$  binary glasses are well-known from previous  $^{29}\text{Si}$  NMR studies of Mg-silicate glasses and crystals and from *ab initio* chemical shift calculations to be  $\sim -66$ ,  $-75$ , and  $-82\ \text{ppm}$ , respectively.<sup>11,14–16</sup> In this work, Gaussian peaks have been used to represent the  $^{29}\text{Si}$  MAS NMR line shapes of  $\text{Q}^0$ ,  $\text{Q}^1$ , and  $\text{Q}^2$  species. The  $\delta_{\text{iso}}$  values for the  $\text{Q}^0$ ,  $\text{Q}^1$ , and  $\text{Q}^2$  species have been kept constrained to within  $\pm 1\ \text{ppm}$  of the above-mentioned values, and the corresponding peak widths  $\Delta$  (full width at half-maximum) were found to vary within the narrow ranges of 7–9, 9–11, and 10–12 ppm,

**TABLE 1: Isotropic Shift ( $\delta_{\text{iso}}$ ) and Full Width at Half-Maximum ( $\Delta$ ) for Different  $Q^n$  Species as Obtained from Simulation of the  $^{29}\text{Si}$  MAS NMR Spectra of the  $(\text{MgO})_x(\text{SiO}_2)_{100-x}$  Glasses<sup>a</sup>**

$x$	$Q^0$		$Q^1$		$Q^2$		$Q^3$		$Q^4$	
	$\delta_{\text{iso}}$ (ppm)	$\Delta$ (ppm)	$\delta_{\text{iso}}$ (ppm)	$\Delta$ (ppm)	$\delta_{\text{iso}}$ (ppm)	$\Delta$ (ppm)	$\delta_{\text{iso}}$ (ppm)	$\Delta$ (ppm)	$\delta_{\text{iso}}$ (ppm)	$\Delta$ (ppm)
50			-74.9	11.7	-83.9	12.6	-94.2	13.2	-107.2	14.9
52			-75.0	11.0	-84.0	11.7	-94.2	13.0		
54	-65.5	9.7	-75.8	10.9	-84.1	11.1	-92.8	10.0		
56	-65.5	8.0	-74.7	11.0	-82.7	10.0	-92.2	13.0		
58	-65.5	7.5	-74.5	9.0	-82.0	10.1				
60	-67.5	7.0	-75.0	9.0	-82.0	10.0				
62	-67.5	9.0	-75.0	10.1	-82.5	10.0				
64	-67.5	7.0	-74.5	9.0						
66.7										

<sup>a</sup> The error associated with both  $\delta_{\text{iso}}$  and  $\Delta$  is  $\pm 1$  ppm.

respectively, for all glasses. The  $^{29}\text{Si}$  MAS NMR spectra of glasses with  $\leq 56\%$  MgO required the fitting of an additional peak centered at a  $\delta_{\text{iso}}$  value of  $-92 \pm 2$  ppm for  $Q^3$  species whose  $\Delta$  was found to vary between 12 and 14 ppm. This value of  $\delta_{\text{iso}}$  for  $Q^3$  species is in good agreement with those reported in the literature for  $Q^3$  species in a wide range of crystalline alkali and alkaline-earth silicates.<sup>15,17</sup> In addition, simulation of the  $^{29}\text{Si}$  MAS NMR spectrum of the glass with 50% MgO required consideration of the presence of a small fraction of  $Q^4$  species. The corresponding peak was found to be located at a  $\delta_{\text{iso}}$  value of  $-107.2$  ppm, again consistent with similar values reported in the literature for  $Q^4$  species in crystalline alkaline-earth silicates.<sup>15</sup> The simulation parameters for all  $^{29}\text{Si}$  MAS NMR spectra are listed in Table 1, and some typical fits are shown in Figure 2. The relatively high values of  $\Delta$  for the  $Q^3$  and  $Q^2$  species compared to those for the  $Q^0$  and  $Q^1$  species (Table 1) are consistent with similar observations made by Larson et al. in a recent  $^{29}\text{Si}$  MAS NMR study of binary Li-silicate glasses with high  $\text{Li}_2\text{O}$  contents of up to 64.3 mol %.<sup>18</sup> The relative fractions of various  $Q$  species have been obtained by integrating the respective component line shapes and are listed in Table 2 for all glass compositions, and their compositional variations are shown in Figure 3.

The  $^{25}\text{Mg}$  MAS NMR spectra, collected for select glasses in the series, are shown in Figure 4. These spectra are all

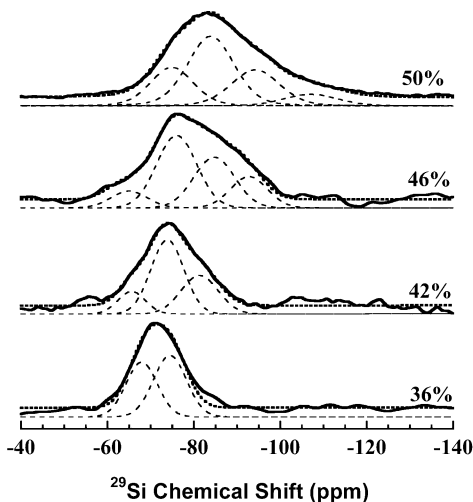


**Figure 2.** Examples of typical fits of  $^{29}\text{Si}$  MAS NMR spectra of  $(\text{MgO})_x(\text{SiO}_2)_{100-x}$  glasses. Corresponding glass compositions are given alongside each spectrum in terms of  $\text{SiO}_2$  content in mol %. Experimental and simulated spectra are shown with solid and dotted lines, respectively. Individual simulation components corresponding to different  $Q^n$  species are shown as dashed lines (Gaussian peaks).

**TABLE 2: Relative Fraction (Percentages) of Different  $Q^n$  Species as Obtained from Simulation of the  $^{29}\text{Si}$  MAS NMR Spectra of the  $(\text{MgO})_x(\text{SiO}_2)_{100-x}$  Glasses**

$x$	% $Q^0$	% $Q^1$	% $Q^2$	% $Q^3$	% $Q^4$
50	0.0	25.0	42.0	25.7	7.3
52	0.0	39.0	48.0	13.0	0.0
54	6.0	47.0	31.0	16.0	0.0
56	10.0	58.0	26.0	6.0	0.0
58	14.5	54.3	31.2	0.0	0.0
60	27.5	58.0	14.5	0.0	0.0
62	40.0	52.0	8.0	0.0	0.0
64	50.0	50.0	0.0	0.0	0.0
66.7	60.0	40.0	0.0	0.0	0.0

characterized by a broad, asymmetric line shape with a high-field tail and a peak maximum located near  $\sim -20$  ppm. These  $^{25}\text{Mg}$  MAS NMR spectra are typical of a powder pattern for central transition of a quadrupolar nuclide with second-order quadrupolar broadening resulting from a distribution of quadrupolar parameters. The  $^{25}\text{Mg}$  MAS NMR spectrum of the  $\text{MgSiO}_3$  glass in Figure 4 is consistent with that reported by Shimoda et al. in earlier studies on isotopically enriched (99%  $^{25}\text{Mg}$ ) glasses.<sup>12,13</sup> The high-resolution  $^{25}\text{Mg}$  3QMAS NMR spectrum of this glass was interpreted by Shimoda et al. to represent  $\text{Mg}^{\text{VI}}$  sites in 6-fold coordination with oxygen with at least four different types of such sites in the glass characterized by  $\delta_{\text{iso}}$  ranging between 1 and 24 ppm and quadrupolar product  $P_Q$  ranging between 3.3 and 7.3 MHz, implying a wide range of site distortions. The  $\delta_{\text{iso}}$  of  $\text{Mg}^{\text{VI}}$  sites in silicates ranges

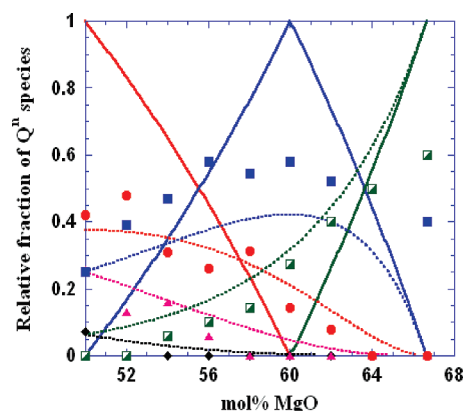


**Figure 3.** Compositional variation of relative fractions of different  $Q^n$  species (symbols) as obtained from simulation of the  $^{29}\text{Si}$  MAS NMR spectra of the  $(\text{MgO})_x(\text{SiO}_2)_{100-x}$  glasses. The black, pink, red, blue, and green colored symbols correspond to  $Q^4$ ,  $Q^3$ ,  $Q^2$ ,  $Q^1$ , and  $Q^0$  species, respectively. Solid and dashed lines with corresponding colors denote compositional variation of  $Q^n$  species according to the predictions of binary and statistical distribution models, respectively.



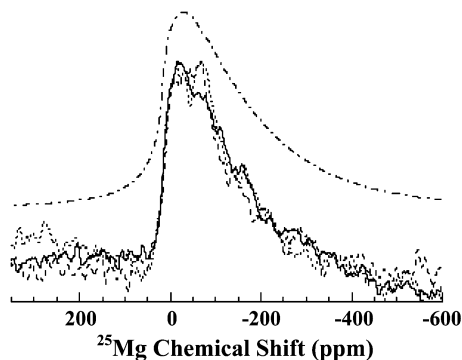


**Figure 4.**  $^{25}\text{Mg}$  MAS NMR spectra of  $(\text{MgO})_x(\text{SiO}_2)_{100-x}$  glasses with 50 (dotted line), 40 (dashed line), and 33.3 (solid line) mol %  $\text{SiO}_2$ . The topmost line shape shown with the dot-dashed line represents simulation with a Gaussian distribution of  $C_Q$  and  $\eta$  values. See text for simulation parameters. The line shape simulation program QuadFit<sup>25</sup> was used for this simulation.

between  $\sim 5$  and 15 ppm, while  $\delta_{\text{iso}}$  is  $\sim 50$  ppm for 4-fold coordinated  $\text{Mg}^{\text{IV}}$  sites. Although  $\delta_{\text{iso}}$  for 5-fold coordinated  $\text{Mg}^{\text{V}}$  sites is not known, it is expected to be situated somewhere between 15 and 50 ppm. Shimoda et al. has therefore suggested that one of the four Mg sites in  $\text{MgSiO}_3$  glass, characterized by the highest value of  $\delta_{\text{iso}} = 24$  ppm, may in fact be a  $\text{Mg}^{\text{V}}$  site.<sup>12</sup>

The  $^{25}\text{Mg}$  MAS NMR spectra shown in Figure 4 can be simulated reasonably well with a second-order quadrupolar powder pattern with a Gaussian distribution of quadrupolar parameters. The best fit in all cases yields mean values of  $\sim 17$  ppm for  $\delta_{\text{iso}}$ ,  $\sim 7.6$  MHz for the quadrupolar coupling constant  $C_Q$ , and  $\sim 0.35$  for the asymmetry parameter  $\eta$  (Figure 4). The corresponding widths of the distributions for  $C_Q$  and  $\eta$  are 3 MHz and 0.1, respectively. Although the  $\delta_{\text{iso}}$  value of 17 ppm can be safely assigned to  $\text{Mg}^{\text{VI}}$  sites in 6-fold coordination with oxygen,<sup>19</sup> as noted earlier by Shimoda et al.,<sup>12</sup> the possibility of the presence of some fraction of  $\text{Mg}^{\text{V}}$  sites in these glasses cannot be entirely discarded. It is also important to note the strong similarity between the  $^{25}\text{Mg}$  MAS NMR line shapes in Figure 4 that implies that the average coordination number of Mg in these glasses remains unchanged irrespective of composition.

#### IV. Discussion

One extreme of the Q species distribution in silicate glasses is defined by the binary distribution that assumes sequential conversion of Q species:  $\text{Q}^n \rightarrow \text{Q}^{n-1}$  with increasing concentration of network modifiers. The binary distribution predicts the presence of at the most two types of Q species, i.e.,  $\text{Q}^n$  and  $\text{Q}^{n-1}$ , for any particular composition. The other extreme of Q species distribution is based on a purely statistical model that assumes a random modification of a fully connected Si–O network via formation of nonbridging oxygens (NBOs) in the glass structure upon addition of network modifying cations.<sup>20–22</sup> The relative concentrations of the  $\text{Q}^n$  species in glasses along the pseudobinary join  $\text{MgSiO}_3\text{--Mg}_2\text{SiO}_4$  as determined in this study (Figure 3) fall between these two extremes, in agreement with the results of previous  $^{29}\text{Si}$  MAS NMR studies of Q speciation in a wide range of binary silicate glasses.<sup>18,20,22</sup> However, the deviation of Q species distribution from a simple binary model in these Mg-silicate glasses is unusually strong and in fact glasses with  $<64\%$  MgO show a closer correspondence with the predictions of the statistical model (Figure 3). The deviation of Q speciation from the binary model can be expressed in terms of disproportionation reactions such as

**TABLE 3: Equilibrium Constants  $k_n$  of the  $\text{Q}^n$  Species Disproportionation Reaction (See Text for Details) in Different  $(\text{MgO})_x(\text{SiO}_2)_{100-x}$  Glasses<sup>a</sup>**

$x$	$k_1$	$k_2$	$k_3$
50		0.364	0.464
52		0.220	
54	0.084	0.782	
56	0.077	0.515	
58	0.153		
60	0.118		
62	0.118		
64			
66.7			
$\text{CaSiO}_3$ <sup>17</sup>	0.105	0.156	0.106
$\text{Li}_2\text{O--SiO}_2$ <sup>18,23</sup>	0.062*, 0.258*	0.30, 0.044*, 0.088*	0.08, 0.055*
$\text{Na}_2\text{O--SiO}_2$ <sup>23</sup>	0.14	0.06	0.02
$\text{K}_2\text{O--SiO}_2$ <sup>23</sup>	0.02	0.01	0.01

<sup>a</sup> Previously published values of  $k_n$  for other alkali and alkaline-earth silicate glasses are included for comparison. Values of  $k_n$  with an asterisk are from ref 18.

$2\text{Q}^n = \text{Q}^{n-1} + \text{Q}^{n+1}$  ( $1 \leq n \leq 3$ ). This disproportionation reaction shifts to the right with increasing cooling rate of the glass and with increasing field strength, i.e., the charge/radius ratio, of the modifier cation.<sup>22</sup> A more quantitative comparison can be made if one considers the equilibrium constant of the disproportionation reaction at the glass transition/fictive temperature that can be written as  $k_n = [\text{Q}^{n-1}][\text{Q}^{n+1}]/[\text{Q}^n]^2$ . The  $k_1$ ,  $k_2$ , and  $k_3$  values for different Mg-silicate glass compositions as determined in this study are listed in Table 3 and are compared with the published values for alkali silicates, and  $\text{CaSiO}_3$  glass.<sup>17,18,23</sup> It is clear that Mg-silicate glasses are characterized by some of the highest values of these equilibrium constants ever reported in the literature for binary silicate glasses. These high  $k_n$  values and the significant deviation of the Q species distribution in Mg-silicate glasses from that predicted by a binary model is consistent with the high field strength of  $\text{Mg}^{2+}$  and fast quench rates (i.e., high fictive temperatures) employed in the syntheses of these glasses (Figure 3, Table 3).

Addition of each mole of MgO to  $\text{SiO}_2$  is expected to create 2 mol of NBO according to the reaction  $\text{MgO} + \text{Si--O--Si} = (2 \text{ Si--}\text{O})\cdots\text{Mg}$ , where  $\text{O}$  represents an NBO. Therefore, the total number of NBO atoms per Si (NBO/Si) is fixed by the glass composition. The NBO/Si can also be calculated from the Q speciation result as  $\text{NBO/Si} = \sum x_n(1 - n)$ , where  $x_n$  is the relative fraction of  $\text{Q}^n$  species. A comparison between the expected NBO/Si from glass composition and that obtained from the Q speciation measured by  $^{29}\text{Si}$  MAS NMR for these Mg-silicate glasses is shown in Figure 5. The expected and measured NBO/Si are in reasonably good agreement for all glass compositions except for the  $\text{Mg}_2\text{SiO}_4$  glass where the expected  $\text{NBO/Si} = 4$  is significantly larger compared to the experimental value of 3.6 (Figure 5). Clearly, this deviation is a result of the presence of  $\sim 40\%$  of the Si as  $\text{Q}^1$  species in the end member  $\text{Mg}_2\text{SiO}_4$  composition. The presence of such dimers in this composition is consistent with previous reports of Q speciation in this composition by us and others.<sup>8,11</sup> The formation of  $\text{Q}^1$  species in the  $\text{Mg}_2\text{SiO}_4$  glass implies that “free” oxygen ions are released from disproportionation reactions that can be written as  $2\text{Q}^0 = 2\text{Q}^1 + \text{O}^{2-}$ . These “free” oxygen ions are expected to be charge balanced by and bonded to  $\text{Mg}^{2+}$  ions in the structure, as is indeed observed in the high-pressure polymorph of the mineral forsterite ( $\text{Mg}_2\text{SiO}_4$ ), known as wadsleyite.<sup>24</sup> In the structure of wadsleyite characterized by tetrahedrally coordinated Si present as  $\text{Q}^1$  species, the “free” oxygen ions

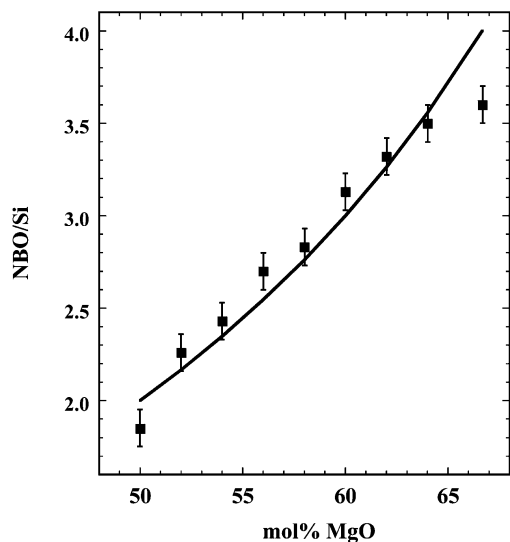


**Figure 5.** Comparison of the experimental (symbols) and calculated (from glass composition: solid line) number of nonbridging oxygens per Si atom in  $(\text{MgO})_x(\text{SiO}_2)_{100-x}$  glasses.

are shared by  $\text{MgO}_6$  octahedra. The  $^{29}\text{Si}$  and  $^{25}\text{Mg}$  MAS NMR spectra presented here conclusively indicate that the structure of  $\text{Mg}_2\text{SiO}_4$  glass is characterized by a mixture of  $\text{Q}^0$  and  $\text{Q}^1$  species (see Table 2) and  $\text{MgO}_6$  octahedra, and therefore, the nearest-neighbor bonding environments in this glass may look locally similar to that of a mixture of wadsleyite and forsterite phases.

When taken together, these results indicate a structural scenario where the Mg-silicate glasses with  $\geq 60$  mol % MgO can be stabilized by the formation of a network of interconnected  $\text{SiO}_4$  and  $\text{MgO}_6$  polyhedra where the  $\text{SiO}_4$  tetrahedra are present as  $\text{Q}^0$  and  $\text{Q}^1$  species. A simple bond-valence argument indicates that in an interconnected network of  $\text{SiO}_4$  and  $\text{MgO}_6$  polyhedra each Si–NBO atom is expected to be shared by three Mg atoms, as is indeed observed in the crystal structures of forsterite and wadsleyite polymorphs of  $\text{Mg}_2\text{SiO}_4$ .<sup>24</sup> This structural scenario is different from that proposed by Kohara et al. for the stabilization of the  $\text{Mg}_2\text{SiO}_4$  glass which was suggested to be due to the formation of the percolation domain of interconnected  $\text{MgO}_x$  ( $x = 4, 5, 6$ ) polyhedra where 4 and 5 coordinated Mg sites dominate the structure.<sup>10</sup> On the other hand, Shimoda et al. ascribed the glass formation ability of the invert glasses to the formation of a sparse tetrahedral  $(\text{Si},\text{Mg})\text{O}_4$  network structure.<sup>12,13</sup> However, the  $^{25}\text{Mg}$  MAS NMR results presented here indicate that Mg is predominantly 6-fold coordinated in all invert Mg-silicate glasses. Although the presence of some fraction of 5-fold coordinated Mg sites in these glasses cannot be ruled out, the possibility of the presence of any significant fraction of tetrahedrally coordinated  $\text{Mg}^{\text{IV}}$  sites can be safely discarded. Therefore, the existence of a tetrahedral  $(\text{Si},\text{Mg})\text{O}_4$  network is not tenable as a hypothesis for the structure of invert Mg-silicate glasses. Finally, the strong similarity between the  $^{25}\text{Mg}$  MAS NMR line shapes of invert Mg-silicate glasses over the entire composition range studied here directly contradicts the conclusion of Wilding and co-workers made on the basis of diffraction results that the average coordination number of Mg increases abruptly near the  $\text{Mg}_2\text{SiO}_4$  composition.<sup>6,7</sup> Such discrepancy may result from the fact that these authors determined the Mg–O coordination number by integrating to the first minimum in the pair distribution function. Such a short cutoff distance may result in incorrect coordination numbers in the case of the presence of a mixture of short and long Mg–O bonds with relative ratios that are dependent on composition.

## V. Summary

The  $^{29}\text{Si}$  MAS NMR spectra of glasses along the pseudobinary join  $\text{MgSiO}_3\text{--Mg}_2\text{SiO}_4$  indicate a smooth evolution of the Q species distribution with composition. The Q species distribution falls between the predictions of binary and statistical models and corresponds more closely with the statistical model. This result is consistent with the high fictive temperatures of these glasses and especially the high field strength of  $\text{Mg}^{2+}$  cations. The  $\text{Mg}_2\text{SiO}_4$  end member shows a large deviation in Q speciation from the binary and statistical models and an anomalous presence of a large fraction of  $\text{Q}^1$  dimer species. This result implies the existence of “free oxygen” ions in the glass that are bonded only to  $\text{Mg}^{2+}$  ions, forming Mg–O–Mg bridges.  $^{25}\text{Mg}$  MAS NMR results indicate the presence of  $\text{Mg}^{2+}$  ions predominantly in octahedral coordination in all glasses. The ability of glass formation in this system is possibly dictated by the presence of multiple Q species in glasses with  $<60$  mol % MgO. In contrast, the presence of a network of interconnected  $\text{MgO}_6$  and  $\text{SiO}_4$  polyhedra allows glass formation in compositions with higher MgO content. Furthermore, the “free” oxygens in the  $\text{Mg}_2\text{SiO}_4$  glass provide connectivity to the  $\text{MgO}_6$  polyhedra via Mg–O–Mg bridges that may also contribute to the glass stability.

**Acknowledgment.** The authors wish to thank Mr. N. K. Nasikas (Dept. of Material Sciences, Univ. of Patras) for his help with the  $\text{CO}_2$  melting/quenching experiments, Dr. V. Drakopoulos (ICE/HT-FORTH) for the XRD and EDS measurements, and Dr. M. Orkoulou (Dept. of Pharmacy, Univ. of Patras) for the chemical analysis by atomic absorption. The authors also wish to thank Ms. Mariko Ando, Dr. Yasuto Noda, and Mr. Itaru Oikawa (Graduate School of Engineering, Tohoku University) for their help with the  $^{25}\text{Mg}$  NMR data acquisition. We express our gratitude to M. Tansho and T. Shimizu of NIMS for offering an opportunity to conduct the ultrahigh field NMR experiments. The kind financial support to one of us (G.N.P.) from the Executive Board of FORTH is acknowledged. S.S. was supported by the National Science foundation grant DMR0906070.

## References and Notes

- (1) Helfrich, G. S.; Wood, B. J. *Nature* **2001**, 412, 501.
- (2) Mysen, B.; Richet, P. *Silicate Glasses and Melts: Properties and Structure*; Elsevier B.V.: Amsterdam, The Netherlands, 2005.
- (3) Rawson, H. *Glasses and Their Applications*; Royal Institute of Metals: London, 1991.
- (4) Shelby, J. E. *Introduction to Glass Science and Technology*; Cambridge: RSC, 2005.
- (5) Petricevic, V.; Seas, A.; Alfano, R. R. *Opt. Lett.* **1991**, 16, 811.
- (6) Wilding, M. C.; Benmore, C. J.; Tangeman, J. A.; Sampath, S. *Chem. Geol.* **2004**, 213, 281.
- (7) Wilding, M. C.; Benmore, C. J.; Tangeman, J. A.; Sampath, S. *Europhys. Lett.* **2004**, 67, 212.
- (8) Kalampounias, A. G.; Nasikas, N. K.; Papatheodorou, G. N. *J. Chem. Phys.* **2009**, 131, 114513.
- (9) Tangemann, J. A.; Phillips, B. L.; Navrotsky, A.; Weber, J. K. R.; Hixson, A. D.; Key, T. S. *Geophys. Res. Lett.* **2001**, 28, 2517.
- (10) Kohara, S.; Suzuya, K.; Takeuchi, K.; Loong, C.-K.; Grimsditch, M.; Weber, J. K. R.; Tangeman, J. A.; Key, T. S. *Science* **2004**, 303, 1649.
- (11) Sen, S.; Tangeman, J. A. *Am. Mineral.* **2008**, 93, 946.
- (12) Shimoda, K.; Tobu, Y.; Hatakeyama, M.; Nemoto, T.; Saito, K. *Am. Mineral.* **2007**, 92, 695.
- (13) Shimoda, K.; Nemoto, T.; Saito, K. *J. Phys. Chem. B* **2008**, 112, 6947.
- (14) Gaudio, S. J.; Sen, S.; Leshner, C. E. *Geochim. Cosmochim. Acta* **2008**, 72, 1222.
- (15) Stebbins, J. F. In *Mineral Physics and Crystallography: Handbook of Physical Constants*; Ahren, T. J., Ed.; AGU Reference Shelf: Washington, DC, 1995; p 303.

- (16) Ashbrook, S. E.; Le Polle, L.; Pickard, C. J.; Berry, A. J.; Wimperis, S.; Farnan, I. *Phys. Chem. Chem. Phys.* **2007**, 9, 1587.
- (17) Zhang, P.; Grandinetti, P. J.; Stebbins, J. F. *J. Phys. Chem. B* **1997**, 101, 4004.
- (18) Larson, C.; Doerr, J.; Affatigato, M.; Feller, S.; Holland, D.; Smith, M. E. *J. Phys.: Condens. Matter* **2006**, 18, 11323.
- (19) Kroeker, S.; Stebbins, J. F. *Am. Mineral.* **2000**, 85, 1459.
- (20) Eckert, H. *Prog. Nucl. Magn. Reson. Spectrosc.* **1992**, 24, 159.
- (21) Lacy, E. D. *Phys. Chem. Glasses* **1967**, 8, 238.
- (22) Greaves, G. N.; Sen, S. *Adv. Phys.* **2007**, 56, 1.
- (23) Maekawa, H.; Maekawa, T.; Kawamura, K.; Yokokawa, T. *J. Non-Cryst. Solids* **1991**, 127, 53–64.
- (24) Horiuchi, H.; Sawamoto, H. *Am. Mineral.* **1981**, 66, 568.
- (25) Kemp, T. F.; Smith, M. E. *Solid State NMR* **2009**, 35, 243.

JP9079603